Lough, S., Burns, A., & Watt, G. D. (1983) *Biochemistry 22*, 4062.
Morgan, T. V., Stephens, P. J., Devlin, F., Stout, C. D., Melis, K. A., & Burgess, B. K. (1984) *Proc. Natl. Acad. Sci. U.S.A. 81*, 1931.
Mortensen, L. E., & Thorneley, R. N. F. (1979) *Annu. Rev. Biochem. 48*, 387.
Palmer, G., Multani, J. S., Cretney, W. C., Zemft, W. B., & Mortenson, L. E. (1972) *Arch. Biochem. Biophys. 153*, 328.
Robson, R. L. (1979) *Biochem. J. 181*, 569.
Scherings, G., Haaker, H., Wassink, H., & Veeger, C. (1983) *Eur. J. Biochem. 135*, 599.
Simpson, F., & Burris, R. H. (1983) in *Advances in Nitrogen Fixation Research* (Veeger, C., & Newton, W. E., Eds.) p 243, Nijhoff and Junk Publishers, The Hague, The Netherlands.
Watt, G. D. (1979) *Anal. Biochem. 99*, 399.
Watt, G. D., Burns, A., Lough, S., & Tennent, D. L. (1980a) *Biochemistry 19*, 4926.
Watt, G. D., Burns, A., & Lough, S. (1980b) in *Nitrogen Fixation* (Newton, W. E., & Orme-Johnson, W. H., Eds.) Vol. 1, p 159, University Park Press, Baltimore, MD.
Watt, G. D., Burns, A., & Tennent, D. L. (1981) *Biochemistry 20*, 7272.
Wherland, S., Burgess, B. K., Stiefel, E. I., & Newton, W. E. (1981) *Biochemistry 20*, 5132.
Wong, P. P., & Burris, R. H. (1972) *Proc. Natl. Acad. Sci. U.S.A. 69*, 672.

Functional and Immunochemical Characterization of a Mutant of *Escherichia coli* Energy Uncoupled for Lactose Transport

Doris Herzlinger,[‡] Nancy Carrasco, and H. Ronald Kaback*

Department of Biochemistry, Roche Institute of Molecular Biology, Roche Research Center, Nutley, New Jersey 07110
Received July 9, 1984

ABSTRACT: Right-side-out cytoplasmic membrane vesicles from *Escherichia coli* ML 308-22, a mutant "uncoupled" for β-galactoside/H^+ symport [Wong, P. T. S., Kashket, E. R., & Wilson, T. H. (1970) *Proc. Natl. Acad. Sci. U.S.A. 65*, 63], are specifically defective in the ability to catalyze accumulation of methyl 1-thio-β-D-galactopyranoside (TMG) in the presence of an H^+ electrochemical gradient (interior negative and alkaline). Furthermore, the rate of carrier-mediated efflux under nonenergized conditions is slow and unaffected by ambient pH from pH 5.5 to 7.5, and TMG-induced H^+ influx is only about 15% of that observed in vesicles containing wild-type *lac* permease (ML 308-225). Alternatively, ML 308-22 vesicles bind *p*-nitrophenyl α-D-galactopyranoside and monoclonal antibody 4B1 to the same extent as ML 308-225 vesicles and catalyze facilitated diffusion and equilibrium exchange as well as ML 308-225 vesicles. When entrance counterflow is studied with external substrate at saturating and subsaturating concentrations, it is apparent that the mutation simulates the effects of deuterium oxide [Viitanen, P., Garcia, M. L., Foster, D. L., Kaczorowski, G. J., & Kaback, H. R. (1983) *Biochemistry 22*, 2531]. That is, the mutation has no effect on the rate or extent of counterflow when external substrate is saturating but stimulates the efficiency of counterflow when external substrate is below the apparent K_m. Moreover, although replacement of protium with deuterium stimulates counterflow in ML 308-225 vesicles when external substrate is subsaturating, the isotope has no effect on the mutant vesicles under the same conditions. It is suggested that the mutation in ML 308-22 results in a *lac* permease molecule with a higher pK_a, thereby either limiting the rate of deprotonation or altering the equilibrium between protonated and deprotonated forms of the carrier. Although antibody 4B1 binds identically with ML 308-225 and ML 308-22 vesicles, monoclonal antibody 4A10R, which is directed against a cytoplasmically disposed epitope in the permease that is partially related to the carboxyl terminus of the molecule, binds to inside-out vesicles from the mutant only 30% as well as it binds to the same preparation from ML 308-225. Since the ultimate carboxyl terminus of the permease does not play a direct role in catalytic activity [Carrasco, N., Herzlinger, D., Mitchell, R., DeChiara, S., Danho, W., Gabriel, T. F., & Kaback, H. R. (1984) *Proc. Natl. Acad. Sci. U.S.A. 81*, 4672], it is concluded that the mutation in ML 308-22 probably does not occur in the carboxyl terminus of the permease but causes a conformational change in this region of the molecule.

The *lac* carrier protein (i.e., *lac* permease), the product of the *lac y* gene in *Escherichia coli*, has been solubilized from the cytoplasmic membrane, purified to homogeneity in a completely functional state, and demonstrated to be the only polypeptide required for transport of β-galactosides [cf. Kaback (1983, 1984) and Overath & Wright (1983) for recent reviews]. The permease catalyzes translocation of substrate with H^+ (i.e., symport), and in the presence of a proton electrochemical gradient ($\Delta\bar{\mu}_{H^+}$),[1] it couples the downhill movement

[‡]Present address: Department of Mononuclear Cell Biology, New York Blood Center, New York, NY 10021.

[1] Abbreviations: $\Delta\bar{\mu}_{H^+}$, proton electrochemical gradient; C, carboxyl; TMG, methyl 1-thio-β-D-galactopyranoside; CCCP, carbonyl cyanide *m*-chlorophenylhydrazone; PMS, phenazine methosulfate; *p*-CMBS, *p*-(chloromercuri)benzenesulfonate; diS-C_3-(5), 3,3′-diisopropylthiodicarbocyanine; Dns^6-Gal, 6-(*N*-dansylamino)hexyl 1-thio-β-D-galactopyranoside; NPG, *p*-nitrophenyl α-D-galactopyranoside; RSO, right side out; ISO, inside out; $NaDodSO_4$, sodium dodecyl sulfate; kDa, kilodalton(s).

0006-2960/85/0424-0221$01.50/0

of H^+ to the uphill transport of β-galactosides (i.e., active transport). Conversely, under nonenergized conditions, downhill movement of substrate along a concentration gradient drives uphill transport of H^+ with generation of $\Delta\bar{\mu}_{H^+}$, the polarity of which is determined by the direction of the substrate concentration gradient. As such, the *lac* permease exemplifies a large class of biological machines that couple the energy released from the downhill movement of a cation to another process.

Various approaches are being utilized to study the structure and function of the permease. The protein is a 46.5-kDa polypeptide containing 417 amino acid residues of known sequence (Büchel et al., 1980). On the basis of circular dichroic measurements and an analysis of sequential hydropathic character, a secondary structure model has been proposed suggesting that the protein consists of 12 or 13 hydrophobic segments in an α-helical conformation that traverse the membrane in a zigzag manner connected by more hydrophilic, charged loops (Foster et al., 1983). Although by no means proven, preliminary support for the model has been obtained. Proteolysis experiments with right-side-out (RSO) and inside-out (ISO) cytoplasmic membrane vesicles in which the permease was specifically photolabeled with *p*-nitrophenyl α-D-galactopyranoside demonstrate directly that the protein spans the bilayer (Goldkorn et al., 1983). In addition, binding studies with monoclonal antibodies directed against the purified protein and with site-directed polyclonal antibodies demonstrate that the permease is inserted asymmetrically into the membrane with the carboxyl (C)-terminus exposed on the cytoplasmic surface of the membrane (Seckler et al., 1983; Carrasco et al., 1984a,c) and epitopes for two independent monoclonal antibodies exposed on the periplasmic (i.e., exterior) surface (Carrasco et al., 1982, 1983a,b, 1984c; Herzlinger et al., 1984). One of the monoclonal antibodies (designated 4B1) inhibits those transport reactions that involve net H^+ translocation with little or no effect on equilibrium exchange or on the ability of the permease to bind a high-affinity ligand (Carrasco et al., 1982, 1984b). Furthermore, kinetic studies (Robertson et al., 1980; Ghazi & Shechter, 1981; Viitanen et al., 1984) and radiation inactivation analysis (Goldkorn et al., 1984) are consistent with the hypothesis that $\Delta\bar{\mu}_{H^+}$ may induce a structural alteration in the *lac* carrier (e.g., dimerization). Finally, oligonucleotide-directed, site-specific mutagenesis has been utilized to transform Cys-148 into a glycine residue, and it has been shown that although Cys-148 is required for substrate protection against alkylation by *N*-ethylmaleimide, it is not obligatory for active transport (Trumble et al., 1984).

Although the evidence supporting the conclusion that the *lac* permease catalyzes β-galactoside/H^+ symport is virtually unequivocal, the mechanism of the reaction, particularly the means by which H^+ transport and sugar transport are coupled, is enigmatic. Nonetheless, experiments with RSO membrane vesicles (Kaczorowski & Kaback, 1979; Kaczorowski et al., 1979) and proteoliposomes reconstituted with purified *lac* permease (Garcia et al., 1983; Viitanen et al., 1983) in which passive lactose movements were used to drive turnover of the permease suggest a model in which the overall rate of carrier-mediated lactose efflux down a concentration gradient is limited either by deprotonation of the carrier on the outer surface of the membrane or by a step corresponding to the return of the unloaded carrier to the inner surface of the membrane. The results are also consistent with the following conclusions: (i) efflux occurs by an ordered mechanism in which lactose is released first from the carrier followed by loss of the symported H^+; (ii) the carrier recycles in the protonated state during exchange and counterflow; (iii) reactions catalyzed by the unloaded carrier involve net movement of negative charge.

In another approach, Wong et al. (1970), Wilson & Kutsch (1972), and West & Wilson (1973) described the isolation and some of the properties of certain mutants that are "uncoupled" for H^+/β-galactoside symport. The mutants exhibit unimpaired facilitated diffusion but are specifically defective in their ability to accumulate β-galactosides against a concentration gradient and exhibit decreased β-galactoside-induced H^+ influx under partially deenergized conditions. Moreover, the uncoupled phenotype in *E. coli* X71-54 maps with *lac y* (Wilson & Kutsch, 1972), in the C-terminal third of the gene (Hobson et al., 1977). The experiments described here were initiated to study one of the uncoupled mutants by using the strategy outlined by Kaczorowski & Kaback (1979) and to examine binding of monoclonal antibody 4B1, since this antibody induces alterations in transport that resemble many of those observed in the uncoupled mutants (Carrasco et al., 1982, 1984b).

Experimental Procedures

Materials

[^{14}C]Methyl 1-thio-β-D-galactopyranoside (TMG; 54.7 mCi/mmol) and [U-^{14}C]proline (287 mCi/mmol) were purchased from New England Nuclear. Valinomycin, nigericin, carbonyl cyanide *m*-chlorophenylhydrazone (CCCP), and phenazine methosulfate (PMS) were obtained from CalBiochem, *p*-(Chloromercuri)benzenesulfonate (*p*-CMBS) was from Sigma, deuterium oxide (>99% pure) was from Aldrich Chemical Co., and 3,3′-diisopropylthiodicarbocyanine [diS-C_3-(5)] was from Molecular Probes. 6-(*N*-dansylamino)hexyl 1-thio-β-D-galactopyranoside (Dns^6-Gal) was synthesized as described by Schuldiner et al. (1975), and *p*-nitro[2-^{3}H]phenyl α-D-galactopyranoside (NPG) was synthesized by Yu-Ling Liu (Isotope Synthesis Group, Hoffmann-La Roche, Inc.) under the direction of Arnold Liebman. All other materials were reagent grade and obtained from commercial sources.

Methods

Growth of Cells and Preparation of Membrane Vesicles. *E. coli* ML 30 ($i^+z^+y^+a^+$), ML 308-225 ($i^-z^-y^+a^+$), and ML 308-22 ($i^-z^+y^{unc}a^+$) were grown on minimal medium A (Davis & Mingioli, 1959) containing 1% disodium succinate (hexahydrate). RSO membrane vesicles were prepared by osmotic lysis (Kaback, 1971; Short et al., 1975), and ISO vesicles were prepared by passing cells through a French pressure cell at 5000 psi (Reenstra et al., 1980).

Transport Assays. Respiration-driven accumulation of [^{14}C]TMG or [^{14}C]proline was measured under oxygen with reduced PMS as electron donor (Kaback, 1974). Carrier-mediated [^{14}C]TMG influx and efflux down appropriate concentration gradients in the absence of $\Delta\bar{\mu}_{H^+}$ and TMG-induced H^+ influx were measured as described (Kaczorowski & Kaback, 1979; Kaczorowski et al., 1979; Patel et al., 1982). Entrance counterflow was assessed by measuring TMG efflux-induced enhancement of Dns^6-Gal fluorescence (Schuldiner et al., 1975). Membrane vesicles were concentrated to 40 mg of protein/mL in 100 mM potassium phosphate (pH 6.6)/10 mM magnesium sulfate; valinomycin, nigericin, and TMG were added to final concentrations of 20 μM, 2 μM, and 30 mM, respectively, and the samples were incubated at 25 °C for 3 h. An aliquot of the suspension (2 μL) was then rapidly diluted into 2 mL of 100 mM potassium phosphate

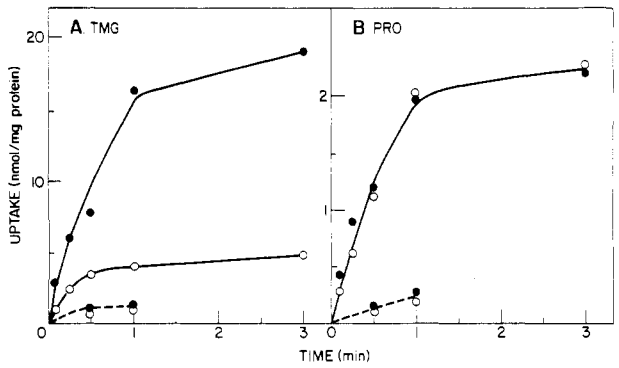

FIGURE 1: Respiration-driven transport of TMG (A) and proline (B). RSO vesicles from *E. coli* ML 308-225 (●) and ML 308-22 (○) (40 μg of membrane protein/sample) in 50 mM potassium phosphate (pH 6.6)/10 mM magnesium sulfate were incubated with 0.4 mM [^{14}C]TMG (27.5 mCi/mmol) (A) or 10 μM [^{14}C]proline (287 mCi/mmol) (B) and assayed for substrate accumulation at the times indicated in the presence (—) or absence (- - -) of reduced PMS as described (Kaback, 1974).

(pH 6.6) and 10 mM magnesium sulfate containing a given concentration of Dns^6-Gal in a 1 × 1 cm quartz cuvette which had been placed in the sample compartment of a Perkin-Elmer MPF4 spectrophotofluorometer. Fluorescence was recorded continuously at 500 nm (excitation 340 nm) with the emission and excitation slits set at 6 nm. The sample chamber of the instrument was maintained at 25 °C with a Lauda Model K-2/R circulating water bath (Brinkmann).

Measurement of Membrane Potential ($\Delta\psi$). $\Delta\psi$ (interior negative) was determined from the steady-state distribution of [^{3}H]tetraphenylphosphonium (Ramos et al., 1979; Felle et al., 1980) and from fluorescence quenching of diS-C_3-(5) (Waggoner, 1979). Valinomycin-mediated potassium diffusion potentials ($K^+_{in} \rightarrow K^+_{out}$) were used for calibration. Fluorescence was monitored at 670 nm, with excitation at 622 nm, and diS-C_3-(5) was used at a final concentration of 1 μM.

Immunochemical Assays. Monoclonal antibodies directed against purified *lac* permease were prepared and iodinated as described (Carrasco et al., 1982; Herzlinger et al., 1984). Site-directed polyclonal IgG directed against a dodecapeptide corresponding in sequence to the C-terminus of the *lac* carrier was prepared and iodinated as described (Carrasco et al., 1984c). Binding assays with RSO and ISO membrane vesicles were performed as described (Herzlinger et al., 1984). Sodium dodecyl sulfate ($NaDodSO_4$)/polyacrylamide gel electrophoresis was carried out as described by Laemmli (1970), and immunoblotting on nitrocellulose (BA85; S&S) was performed electrophoretically for 12 h at constant current (50 mA) (Carrasco et al., 1982).

NPG Binding. Binding of [^{3}H]NPG was measured under nonenergized conditions by flow dialysis (Rudnick et al., 1976).

Protein Determination. Protein was assayed according to Lowry et al. (1951) using crystalline bovine serum albumin as standard.

RESULTS

$\Delta\bar{\mu}_{H^+}$-Driven TMG Accumulation. As shown by Wong et al. (1970), *E. coli* ML 308-22 is specifically defective in the ability to accumulate β-galactosides, a property retained by RSO membrane vesicles incubated in the presence of reduced PMS (Figure 1). Vesicles prepared from the mutant transport TMG at only about 30% of the rate observed in ML 308-225 vesicles, and the steady-state level of TMG accumulation is reduced by about 85% (panel A). Importantly, however, on the basis of an intravesicular volume of 2.2 μL/mg of membrane protein (Barnes & Kaback, 1971), it can be calculated that ML 308-22 vesicles accumulate TMG to an internal concentration about 5-fold higher than that of the external medium. That is, although the mutant vesicles are unable to accumulate TMG nearly as well as the wild type, they are able to establish a small concentration gradient.

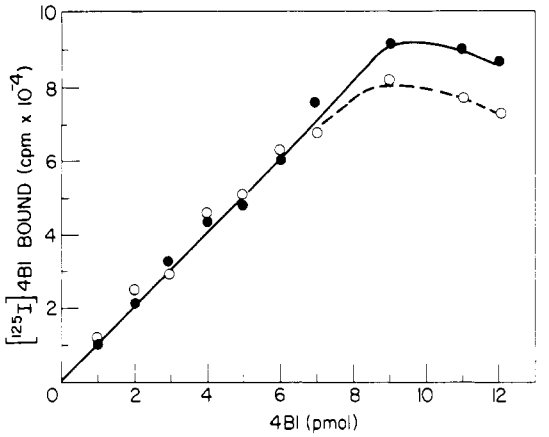

FIGURE 2: Binding of ^{125}I-4B1 to RSO vesicles. RSO vesicles from *E. coli* ML 308-225 (●) and ML 308-22 (○) [46 μg of membrane protein/sample containing about 20 pmol of *lac* permease, as determined by NPG binding (cf. Experimental Procedures)] were incubated in 50 mM potassium phosphate (pH 7.5) containing 5% bovine serum albumin (50 μL final volume) for 1 h at 25 °C. Given amounts of ^{125}I-4B1 were added, and the incubations were continued for 1 h. The samples were then flocculated with poly(L-lysine), filtered, and assayed for bound radioactivity as described (Herzlinger et al., 1984). Data were corrected for nonspecific binding (approximately 5% of input radioactivity) which was determined by incubating the vesicles with a 10-fold molar excess of unlabeled 4B1 relative to *lac* carrier. Specific binding was approximately 75% of input radioactivity.

In contrast, ML 308-22 vesicles catalyze $\Delta\bar{\mu}_{H^+}$-driven proline transport in a manner that is virtually indistinguishable from ML 308-225 vesicles (panel B). Furthermore, although data will not be shown, the $\Delta\bar{\mu}_{H^+}$ generated by ML 308-225 vesicles is similar to that observed in ML 308-22 vesicles, as evidenced by tetraphenylphosphonium distribution measurements (Ramos et al., 1979; Felle et al., 1980) and by fluorescence quenching studies with diS-C_3-(5) (Waggoner, 1979). Phosphoenolpyruvate-dependent methyl α-D-glucopyranoside accumulation (Kaback, 1968) is also identical in ML 308-225 and ML 308-22 vesicles.

Content of lac Permease in ML 308-225 and ML 308-22 Vesicles. Although it has been suggested (Wong et al., 1970) that ML 308-22 has an enhanced level of the *lac* carrier in the membrane, as determined by two independent techniques, membranes from this strain contain a normal complement of permease. (i) Binding of the high-affinity ligand [^{3}H]NPG was determined under nonenergized conditions by flow dialysis (Rudnick et al., 1976), and the specific content of *lac* carrier protein in RSO vesicles from ML 308-225 and ML 308-22 was found to be 0.4 and 0.38 nmol/mg of membrane protein, respectively, assuming that 1 mol of permease binds 1 mol of NPG. (ii) Binding studies with ^{125}I-4B1 yield very similar results (Figure 2). 4B1 is a monoclonal antibody that binds to an epitope in the *lac* carrier disposed on the exterior (periplasmic) surface of the membrane (Carrasco et al., 1982, 1984c; Herzlinger et al., 1984). As shown, binding of ^{125}I-4B1 increases linearly to a maximum and then decreases as unlabeled 4B1, with higher affinity, inhibits binding of ^{125}I-4B1, and the absolute quantity of the epitope present can be approximated from the maximum (Herzlinger et al., 1984). With both preparations, maximum binding occurs at about 9 pmol of 4B1/46 μg of membrane protein. Antibody 4B1

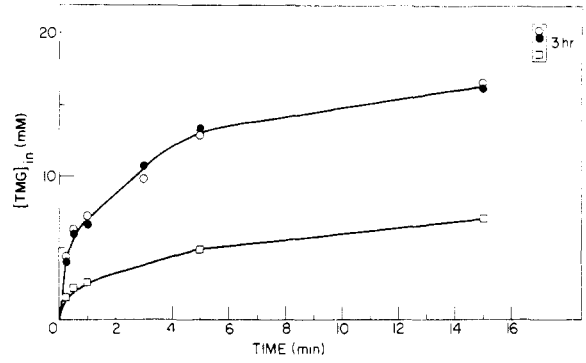

FIGURE 3: Carrier-mediated influx of TMG under nonenergized conditions. RSO vesicles from *E. coli* ML 308-225 (●), Ml 308-22 (○) and uninduced ML 30 (□) were concentrated to 40 mg of protein/mL in 100 mM potassium phosphate (pH 6.6)/10 mM magnesium sulfate, and valinomycin and nigericin were added to final concentrations of 20 and 2 μM, respectively. Influx was initiated by diluting 10 μL of the vesicle suspension into 40 μL of 100 mM potassium phosphate (pH 6.6)/10 mM magnesium sulfate containing 25 mM [^{14}C]TMG (1 mCi/mmol) at 25 °C. Reactions were terminated at the times indicated by adding 5 μL of 200 mM $HgCl_2$ and diluting with 4 mL of 100 mM potassium phosphate (pH 5.5) containing 100 mM LiCl. Samples were filtered immediately on Amicon nitrocellulose filters (0.45-μm pore size) and washed twice with the same quench solution. Radioactivity retained on the filters was determined by liquid scintillation spectrometry. Results similar to those shown for ML 30 vesicles (□) were also obtained with ML 308-225 and ML 308-22 after treatment with 0.3 mM *p*-CMBS (not shown).

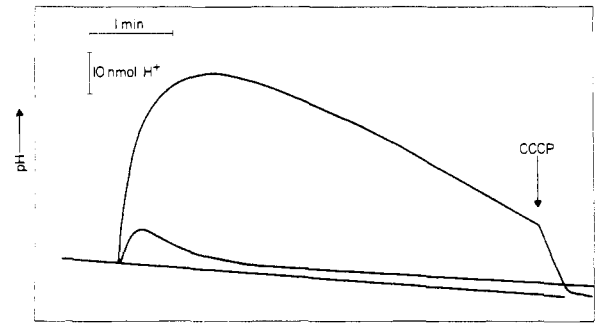

FIGURE 4: TMG-induced H^+ influx. Suspensions of RSO vesicles from *E. coli* ML 308-225 (top tracing), ML 308-22 (middle tracing), and uninduced ML 30 (bottom tracing) (10 mg of protein/mL) in 150 mM KCl/10 mM magnesium sulfate were placed in a closed electrode vessel that was continuously flushed with a stream of water-saturated nitrogen and maintained at 25 °C. Valinomycin was added to a final concentration of 5 μM. The reactions were initiated by addition of TMG to a final concentration of 20 mM, and the pH of the solution was recorded continuously. Where indicated (uppermost tracing), reactions were allowed to proceed for 5 min, when CCCP was added to a final concentration of 20 μM (arrow). The pH changes were calibrated at the end of each experiment by adding 10 μL of 1 mM HCl.

is bivalent, and each mole of IgG binds 2 mol of *lac* carrier protein (Carrasco et al., 1984b; Herzlinger et al., 1984). Therefore, 9 pmol of 4B1 bound indicates that 18 pmol of *lac* carrier is present or, given a molecular weight of 46.5K (Büchel et al., 1980; Newman et al., 1981; Goldkorn et al., 1984), about 0.38 nmol of *lac* carrier protein/mg of membrane protein in both vesicle preparations.

TMG/H$^+$ Symport in the Absence of $\Delta\bar{\mu}_{H^+}$. The experiments presented in Figure 3 represent time courses of TMG influx in nonenergized RSO vesicles treated with valinomycin and nigericin in order to abolish the rate-limiting $\Delta\bar{\mu}_{H^+}$ generated during symport under these conditions (Patel et al., 1982). The time course of TMG equilibration appears to be identical in ML 308-225 and ML 308-22 vesicles. Influx is relatively rapid initially and decreases in rate after about 30 s, and by 15 min, the intravesicular concentration of TMG is about 80% of that of the medium. In contrast, with vesicles from uninduced ML 30, which contain little or no *lac* carrier, the rate of influx is diminished, but eventually, the intravesicular space equilibrates with the medium by means of passive diffusion (Patel et al., 1982); similar results are obtained with ML 308-225 and ML 308-22 vesicles after inactivation of the *lac* carrier with *p*-CMBS.

In a corollary series of experiments, H^+ translocation was measured (Figure 4). When TMG is added to ML 308-225 vesicles, transient alkalinization of the medium is observed, and the pH tracing reaches maximum displacement in about 50 s and returns to the base line after approximately 6 min. Addition of the protonophore CCCP accelerates the rate of return of the tracing to the base line when added after TMG, while addition of CCCP prior to the galactoside abolishes the phenomenon altogether. TMG-induced alkalinization is severely reduced in ML 308-22 vesicles, where the maximum pH shift observed after addition of TMG is only about 15% of that observed in ML 308-225 vesicles.

Efflux of β-galactosides down a concentration gradient is a carrier-mediated process involving H^+ symport (Kaczorowski & Kaback, 1979; Kaczorowski et al., 1979; Garcia et al., 1983; Viitanen et al., 1983). When ML 308-225 vesicles are equilibrated with 30 mM TMG and then diluted into media devoid of TMG, loss of intravesicular TMG is dependent upon the presence of functional *lac* permease, and the rate of efflux increases as a function of pH ($t_{1/2} \simeq$ 110, 70, and 30 s at pH

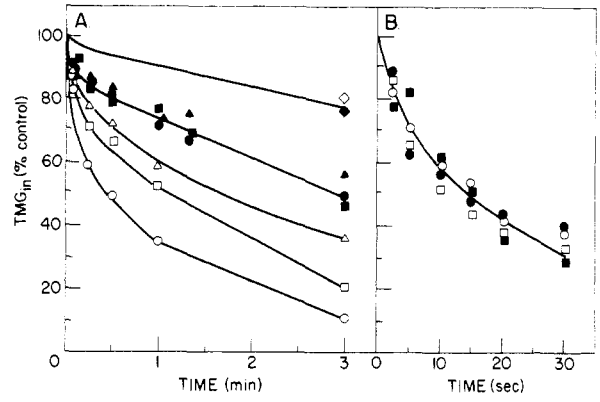

FIGURE 5: TMG efflux (A) and equilibrium exchange (B). (A) Efflux: RSO vesicles from *E. coli* ML 308-225 (open symbols) and ML 308-22 (closed symbols) were concentrated to 40 mg of protein/mL in 100 mM potassium phosphate/10 mM magnesium sulfate at pH 5.5 (△, ▲), 6.6 (□, ■), and 7.5 (○, ●) and at pH 7.5 with 0.3 mM *p*-CMBS (◇, ◆). Valinomycin, nigericin, and [^{14}C]TMG (1 mCi/mmol) were added to final concentrations of 20 μM, 2 μM, and 30 mm, respectively, and the samples were incubated at 25 °C for 3 h. To initiate the reactions, 2-μL aliquots were rapidly diluted into 1 mL of 100 mM potassium phosphate/10 mM magnesium sulfate at the appropriate pH. At the times indicated, $HgCl_2$ was added to a final concentration of 10 mM, and the samples were rapidly diluted with 100 mM potassium phosphate (pH 5.5)/100 mM LiCl and immediately filtered. Data are expressed as a percentage of TMG retained by using zero-time points for normalization. The zero-time values were determined by dilution of vesicles equilibrated with [^{14}C]TMG directly into efflux buffer containing 10 mM $HgCl_2$ followed by immediate dilution and filtration. Absolute values for the zero-time samples were 59.4 nmol/mg of protein ± 15%. Each point represents the average of three independent assays. (B) Exchange: Experiments were performed exactly as described in panel A, except that 30 mM unlabeled TMG was included in the medium into which the equilibrated vesicles were diluted, and the temperature was maintained at 18 °C [cf. Kaczorowski & Kaback, (1979)]. Assays were performed with RSO vesicles from *E. coli* ML 308-225 (open symbols) and ML 308-22 (closed symbols) at pH 5.5 (□, ■) and 7.5 (○, ●). Data are normalized to zero-time values determined as described above, and each point represents the average of three independent assays.

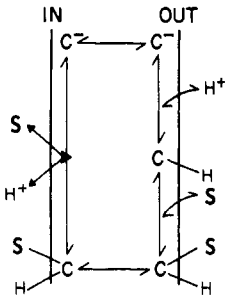

FIGURE 6: Schematic representation of reactions involved in TMG efflux, exchange, and counterflow. C represents the *lac* carrier; S, substrate. The order of substrate binding at the inner surface of the membrane is not implied [from Kaczorowski & Kaback (1979)].

5.5, 6.6, and 7.5, respectively) [Figure 5A; cf. Kaczorowski & Kaback (1979) and Garcia et al. (1983) in addition]. In contrast, the rate of efflux from ML 308-22 vesicles is retarded ($t_{1/2} \simeq 180$ s) and independent of pH.

Exchange. Carrier-mediated efflux down a concentration gradient consists of a minimum of five steps (Figure 6): (1) binding of substrate and H^+ to the carrier on the inner surface of the membrane (order unspecified); (2) translocation of the ternary complex to the outer surface; (3) release of substrate; (4) release of H^+; (5) return of the unloaded carrier to the inner surface (Kaczorowski & Kaback, 1979; Kaczorowski et al., 1979; Garcia et al., 1983; Viitanen et al., 1983; Carrasco et al., 1984b). To determine whether H^+ loss or return of the unloaded carrier is defective in ML 308-22 vesicles, loss of intravesicular [^{14}C]TMG was studied under conditions where the external medium contained equimolar concentrations of unlabeled TMG (i.e., equilibrium exchange). Thus, vesicles equilibrated with 30 mM [^{14}C]TMG were diluted into media containing 30 mM unlabeled TMG, and loss of labeled sugar from the intravesicular space was monitored (Figure 5B). The rate of loss under these conditions is fast ($t_{1/2} \simeq 15$ s) relative to efflux. Strikingly, moreover, the rate of exchange in ML 308-225 and ML 308-22 vesicles is essentially identical at pH 5.5 and pH 7.5. The results imply that the mutant is defective in a step corresponding either to release of H^+ on the outer surface of the membrane or to return of the unloaded carrier, since the rate of translocation is normal when the carrier is fully loaded (cf. Figure 6).

Entrance Counterflow. Entrance counterflow can be utilized to examine the frequency with which the carrier returns from the outer to the inner surface of the membrane in the loaded vs. the unloaded form. At saturating external substrate concentrations, variations in pH (Kaczorowski & Kaback, 1979; Garcia et al., 1983), deuterium oxide (Viitanen et al., 1983), or monoclonal antibody 4B1 (Carrasco et al., 1984b) have no effect on the phenomenon. However, when external substrate is limiting, the C–H form of the carrier on the external surface of the membrane (cf. Figure 6) partitions between two pathways, loss of H^+ and return of the unloaded carrier (efflux) or binding of substrate and return of the loaded carrier (exchange or counterflow). Therefore, when external substrate is limiting, counterflow is progressively inhibited as pH is increased, and efficiency is enhanced by deuterium oxide and by antibody 4B1. Interestingly, the mutation in ML 308-22 mimics the effects of deuterium oxide or antibody 4B1 in this respect (Figure 7). To examine counterflow, ML 308-225 and ML 308-22 vesicles were equilibrated with 30 mM TMG and then diluted 200-fold into medium containing saturating or limiting concentrations of Dns^6-Gal (Schuldiner et al., 1975). The increase in fluorescence at 500 nm probably reflects transport of Dns^6-Gal via the *lac* permease followed by

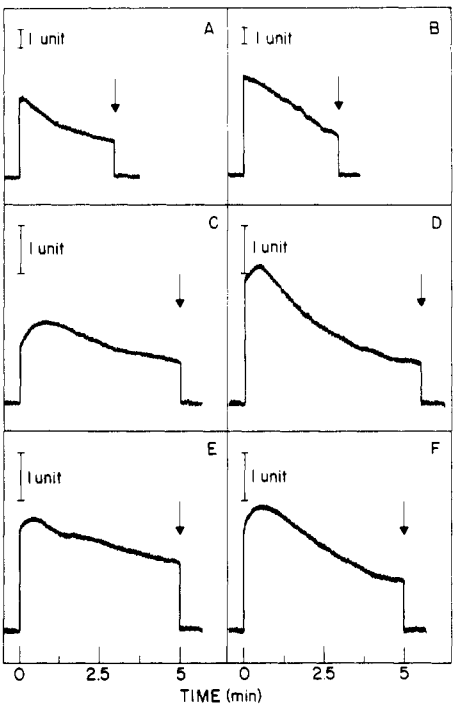

FIGURE 7: TMG/Dns^6-Gal counterflow. RSO vesicles from *E. coli* ML 308-225 (panels A, C, and E) and ML 308-22 (panels B, D, and F) were concentrated to 40 mg of protein/mL in 100 mM potassium phosphate (pH 6.6)/10 mM magnesium sulfate. Valinomycin, nigericin, and TMG were added to final concentrations of 20 μM, 2 μM, and 30 mM, respectively, and the samples were incubated at 25 °C for 3 h. Couterflow at saturating external Dns^6-Gal concentrations [panels A and B; cf. Schuldiner et al. (1975)] was initiated by diluting 2 μL of equilibrated vesicles into 2 mL of 100 mM potassium phosphate (pH 6.6)/10 mM magnesium sulfate containing 20 μM Dns^6-Gal, and fluorescence emission was recorded continuously at 500 nm as described under Experimental Procedures. Arrows designate addition of TMG to a final concentration of 20 mM. Counterflow at subsaturating external Dns^6-Gal concentrations (panels C–F) was performed exactly as described above, except that Dns^6-Gal was present at 5 μM final concentration. In the experiments shown in panels E and F, vesicles were concentrated and equilibrated as described, and the assays were performed exactly as described for panels C and D, except that all solutions were prepared with deuterium oxide in place of H_2O (Viitanen et al., 1983).

nonspecific interaction with the membrane (Overath et al., 1979). At saturating Dns^6-Gal concentrations (i.e., 20 μM), fluorescence increases very rapidly and to similar extents in both vesicle preparations followed by a relatively slow decline to the base line that is rapidly accelerated by addition of 20 mM TMG (Figure 7A,B). With limiting concentrations of Dns^6-Gal (i.e., 5 μM), however, the overshoot is *enhanced* about 2-fold in ML 308-22 vesicles relative to ML 308-225 (compare panels C and D of Figure 7). Finally, as shown previously (Viitanen et al., 1983), deuterium oxide increases the efficiency of counterflow when external substrate is limiting in ML 308-225 vesicles (compare panels C and E), while the isotope has no effect on counterflow in ML 308-22 vesicles (compare panels D and F). In the presence of deuterium oxide, therefore, counterflow profiles in ML 308-225 and ML 308-22 vesicles are comparable at limiting external substrate concentration (compare panels E and F).

Immunochemical Analyses. Recently, the preparation and characterization of monoclonal (Carrasco et al., 1982, 1984b,c; Herzlinger et al., 1984) and site-directed polyclonal (Seckler et al., 1983; Carrasco et al., 1984a,c) antibodies against portions of the *lac* permease have been described. Since monoclonal antibody 4B1 inhibits lactose/H^+ symport in a manner that resembles the effects of the mutation in ML

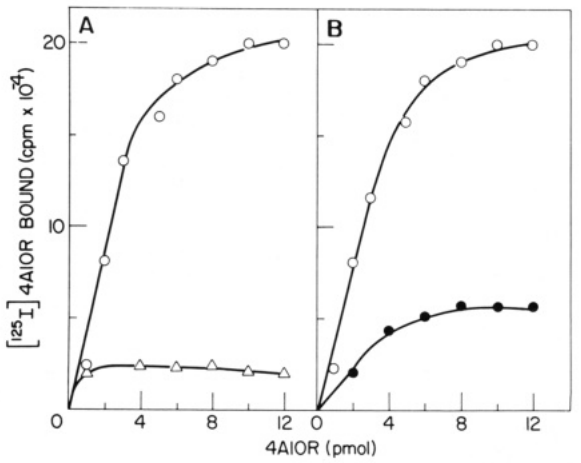

FIGURE 8: Binding of monoclonal antibody 4A1OR. (A) RSO (△) and ISO (○) vesicles from *E. coli* ML 308-225 (46 μg of protein/sample containing approximately 20 pmol of *lac* permease) were incubated in 50 mM potassium phosphate (pH 7.5) containing 5% bovine serum albumin for 1 h. Radioactivity bound to the vesicles and nonspecific binding values were determined as described (Herzlinger et al., 1984). (B) ISO vesicles from *E. coli* ML 308-225 (○) and ML 308-22 (●) were assayed for ^{125}I-4A1OR binding as described in (A).

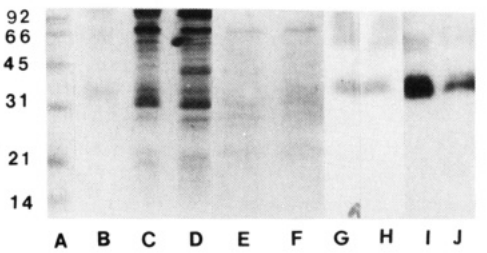

FIGURE 9: Differential binding of antibody 4A1OR to *lac* permease in ML 308-225 and ML 308-22 vesicles as shown by immunoblotting. ISO vesicles from *E. coli* ML 308-225 and ML 308-22 were extracted with 5 M urea, dissolved in $NaDodSO_4$, and electrophoresed on $NaDodSO_4$/15% polyacrylamide gels (25 μg of protein/lane) (Carrasco et al., 1982). Proteins were transferred to nitrocellulose by electroblotting as described under Experimental Procedures. Individual strips of nitrocellulose were then incubated with 100 μg of a given purified monoclonal antibody followed by ^{125}I-labeled protein A (ca. 2×10^5 cpm/strip). Radioautography was carried out at −70 °C overnight. Lanes A–D, Coomassie brilliant blue stained profiles: (A) molecular weight standards; (B) purified *lac* permease; (C) ML 308-225 vesicles; (D) ML 308-22 vesicles. Lanes E and F are amido black stained polypeptide profiles of ML 308-225 and ML 308-22 vesicles, respectively, after transfer to nitrocellulose. Lanes G (ML 308-225 vesicles) and H (ML 308-22 vesicles) are autoradiograms of nitrocellulose treated with antibody 4B1; lanes I and J represent analogous respective samples after treatment with antibody 4A1OR.

308-22, vesicles were tested for their ability to bind 4B1 and other antibodies. Unexpectedly, 4B1 binds normally (cf. Figure 2), but monoclonal antibody 4A1OR exhibits differential binding to ML 308-225 and ML 308-22 vesicles.

Antibody 4A1OR recognizes a cytoplasmically disposed epitope in the protein (Figure 8A). Thus, when ISO and RSO ML 308-225 vesicles containing equivalent amounts of *lac* permease are assayed for 4A1OR binding, it is readily apparent that the antibody binds preferentially to ISO vesicles (i.e., to the cytoplasmic surface). Furthermore, as shown in Figure 8B, binding of ^{125}I-4A1OR to ISO vesicles from ML 308-22 saturates at only about 30% of the value observed with ML 308-225 vesicles.

Additionally, when equivalent amounts of membrane protein from the two vesicle preparations are resolved electrophoretically in $NaDodSO_4$ and tested for antibody binding by immunoblotting, it is observed that antibody 4B1 binds similarly to the bands corresponding to purified *lac* carrier in ML 308-225 and ML 308-22 (Figure 9, compare lanes B, G, and H). Antibody 4A1OR, on the other hand, exhibits significantly decreased binding to the *lac* carrier in ML 308-22 (lane J) relative to ML 308-225 (lane I).

Although the precise nature of the 4A1OR epitope in the *lac* permease is yet to be determined, experiments with site-directed polyclonal antibodies against a dodecapeptide corresponding to the ultimate C-terminus of the protein (Carrasco et al., 1984a,c) suggest that the epitopes for these two classes of IgG are related (Table I). When ISO membrane vesicles from ML 308-225 are incubated with excess anti-C-terminal IgG, followed by incubation with stoichiometric amounts of ^{125}I-4A1OR, binding of the latter is almost completely blocked. Similarly, binding of ^{125}I-anti-C-terminal IgG is blocked by 4A1OR, but the degree of inhibition is not so marked (i.e., 76% vs. 93%). The data imply that the 4A1OR epitope either overlaps with the primary sequence of the C-terminus of the permease or is in close proximity. In either case, binding of anti-C-terminal IgG would be expected to sterically inhibit binding of 4A1OR. Since 4A1OR binds only weakly to C-terminal dodecapeptide, as determined by solid-phase radioimmunoassay (not shown), and binding of ^{125}I-4A1OR is only mildly inhibited by excess C-terminal peptide (Table I), the

Table I: Competitive Binding of Anti-C-Terminal IgG and Antibody 4A10R to ISO Membrane Vesicles from *E. coli* ML 308-225[a]

primary incubation	% antibody bound during secondary incubation	
	^{125}I-4A10R	^{125}I-anti-C
anti-COOH IgG	7	
anti-COOH Fab	24	
COOH-terminal peptide	62	13
4A10R IgG		27

[a] ISO membrane vesicles from *E. coli* ML 308-225 (46 μg of membrane protein containing approximately 20 pmol of *lac* carrier protein) were incubated in 50 mM potassium phosphate (pH 7.5) containing 5% bovine serum albumin for 1 h at room temperature. The samples were then incubated with a 20-fold molar excess of unlabeled Fab or a 10-fold molar excess of IgG or C-terminal peptide relative to *lac* carrier protein in a final volume of 100 μL for 2 h (primary incubation). Saturating amounts of a given competing ^{125}I-labeled IgG were added, and the incubations were continued at 25 °C for another 2 h (secondary incubation). Vesicles were collected and washed by filtration and assayed for bound radioactivity as described (Herzlinger et al., 1984). Nonspecific binding was determined by incubating the vesicles in a 5-fold molar excess of unlabeled IgG prior to incubation with the same labeled antibody. Values for 100% binding were determined by incubating vesicles in ^{125}I-labeled antibody without preincubation; approximately 10 pmol of bivalent IgG was bound per sample.

4A1OR epitope is probably close to but not identical with the C-terminus. Consistently, anti-C-terminal Fab fragments do not block ^{125}I-4A1OR binding as effectively as anti-C-terminal IgG (Table I), and binding of ^{125}I-anti-C-terminal IgG to ISO ML 308-22 vesicles is decreased by only 30% relative to analogous preparations from ML 308-225 (not shown).

Discussion

Transport. The results presented in this paper confirm and extend some of the conclusions presented by Wilson and coworkers (Wong et al., 1970; Wilson & Kutsch, 1972; West & Wilson, 1973) from studies with intact cells. Thus, RSO vesicles from the uncoupled mutant ML 308-22 exhibit a specific defect in the ability to catalyze $\Delta\bar{\mu}_{H^+}$-driven accumulation of TMG (Figure 1) and TMG-induced H^+ influx (Figure 4) but a normal capacity for TMG-facilitated diffusion in the absence of $\Delta\bar{\mu}_{H^+}$ (Figure 3). On a phenomenological level, although the mutated permease is able to translocate

substrate across the membrane, the process is no longer coupled to H^+ translocation. Therefore, the carrier is unable to utilize the energy released from the downhill movement of H^+ in response to $\Delta\bar{\mu}_{H^+}$ to drive uphill accumulation of sugar.

By utilization of an approach initiated by Kaczorowski & Kaback (1979), further insight into the nature of the defect in the mutant has been obtained. It is clear from passive, carrier-mediated efflux experiments that in contrast to the wild-type permease, the uncoupled carrier is defective in two respects (Figure 5A). First, the absolute rate of efflux is slow relative to the wild type; and second, increasing ambient pH from 5.5 to 7.5 has no effect on efflux in ML 308-22 vesicles. Importantly, however, vesicles from the uncoupled mutant carry out equilibrium exchange at the same rate as the wild type, thus demonstrating that the defect does not involve a reaction catalyzed by the loaded carrier (cf. Figure 6). In addition, the demonstration that carrier-mediated efflux is defective in the mutant, while facilitated influx is normal, provides direct evidence that the influx and efflux pathways through the permease under nonenergized conditions cannot be identical [cf. Kaczorowski & Kaback (1979) in addition].

As shown previously (Kaczorowski & Kaback, 1979; Kaczorowski et al., 1979; Garcia et al., 1983; Viitanen et al., 1983; Carrasco et al., 1984b), the frequency with which the permease returns from the outer to the inner surface of the membrane in the loaded vs. the unloaded form can be assessed by studying entrance counterflow. With respect to the mechanism proposed (Figure 6), during counterflow, internal substrate (in this case, TMG) is translocated with H^+ to the outer surface of the membrane where it is released prior to the symported H^+. Depending on the external concentration of substrate (Dns^6-Gal), the resulting C–H (undissociated) form of the permease can partition between two pathways: (1) binding of external substrate and return of the loaded permease, resulting in counterflow (i.e., exchange of internal TMG for external Dns^6-Gal); (2) deprotonation and return of the unloaded permease, resulting in efflux.

With saturating external substrate concentrations, the coupling efficiency for lactose counterflow is 1:1, and the magnitude of the overshoot is independent of pH (Kaczorowski & Kaback, 1979; Garcia et al., 1983) and unaffected by the presence of deuterium oxide (Kaczorowski et al., 1979; Viitanen et al., 1983) or antibody 4B1 (Carrasco et al., 1984b). Therefore, when external substrate is saturating, the vast majority of the permease is presumably turning over in the protonated state (i.e., pathway 1 is favored). In contrast, when counterflow is monitored with external substrate below saturation, coupling efficiency is reduced, and the magnitude of the overshoot is inversely proportional to pH (Kaczorowski & Kaback, 1979; Garcia et al., 1983; Viitanen et al., 1983). Thus, under these circumstances, substrate is released on the surface of the membrane, but binding of external substrate occurs relatively infrequently, allowing deprotonation and return of the unloaded carrier which is reflected by a decrease in counterflow (i.e., pathway 2 is favored). Therefore, any perturbation that favors the undissociated form of the permease, such as replacing protium with deuterium, should increase the efficiency of counterflow when external substrate is present at subsaturating concentrations. With regard to these considerations, it is particularly significant that TMG/Dns^6-Gal counterflow activity in the uncoupled mutant is similar to that observed in the wild type when external Dns^6-Gal is above the apparent K_m and enhanced relative to the wild type when external Dns^6-Gal is below the apparent K_m. Furthermore, although deuterium oxide causes significant stimulation of counterflow activity in wild-type vesicles under the latter conditions (Figure 7C,E), the isotope has no discernible effect on counterflow in ML 308-22 vesicles when external Dns^6-Gal is subsaturating, supporting the notion that the C–H to C^- transition (figure 6) is already slow in the uncoupled mutant.

Taken as a whole, most of the results are consistent with the interpretation that the mutation in ML 308-22 results in a permease molecule with a higher pK_a, thereby causing a decrease in the conversion of C–H to C^- in the overall kinetic cycle shown in Figure 6. Such a mutational event could result readily from a single base change. For example, by changing adenine to guanine in either His codon (CAU or CAC), Arg is encoded (Watson, 1977). Accordingly, the uncoupled permease would bind substrate normally, catalyze all translocation reactions that do *not* involve net H^+ transport (i.e., exchange and counterflow with saturating external substrate concentrations), and manifest enhanced counterflow activity when external substrate is subsaturating. On the other hand, those translocation reactions that involve net H^+ transport would be defective, a prediction documented for $\Delta\bar{\mu}_{H^+}$-driven active transport and carrier-mediated efflux of TMG down a concentration gradient. However, it should be emphasized that despite the temptation to explain the phenomenology in this manner, the interpretation may be overly simplistic. Thus, the uncoupled permease in both intact cells (Wong et al., 1970; Wilson & Kutsch, 1972) and membrane vesicles (Figure 3) appears to catalyze facilitated diffusion at least as well as the wild-type permease. In any event, it seems apparent that cloning and sequencing of *lac* y^{unc} (Brooker & Wilson, 1984) and oligonucleotide-directed, site-specific mutagenesis of specific residues in the *lac* permease (Trumble et al., 1984) should provide insight into the nature of the uncoupled phenotype.

Immunochemistry. As indicated above, one reason for initiating these studies was to examine binding of antibody 4B1 which uncouples lactose/H^+ symport in a manner similar to that described for the mutation in ML 308-22 (Carrasco et al., 1982, 1984a). Although binding of 4B1 to RSO vesicles from ML 308-225 and ML 308-22 is identical within experimental error (Figure 2), monoclonal antibody 4A1OR, which recognizes a cytoplasmically disposed epitope in the *lac* permease (Figure 8A) that is related partially to the C-terminus (Table I), binds to ISO vesicles from ML 308-22 only 30% as well as it binds to the analogous preparation from ML 308-225 (Figure 8b).

In order to discuss the possible implications of the observations, some findings regarding the structure and function of the permease in bacterial membrane vesicles and proteoliposomes should be summarized briefly: (1) Proteoliposomes reconstituted with purified *lac* permease catalyze each of the translocation reactions typical of the β-galactoside transport system with turnover numbers, apparent K_ms, and other kinetic properties that are similar to those observed in RSO vesicles (Kaback, 1983; Viitanen et al., 1984). (2) Antibody 4B1 binds specifically and bivalently to an epitope in the permease that is disposed on the exterior surface of RSO vesicles and reconstituted proteoliposomes (Carrasco et al., 1982, 1984a–c; Herzlinger et al., 1984). (3) The 4B1 epitope is completely unrelated to the C-terminus of the permease (Carrasco et al., 1984c). (4) IgG directed against a dodecapeptide corresponding to the C-terminus of the permease binds almost exclusively to ISO vesicles relative to RSO vesicles, thus demonstrating that the C-terminus is on the inner surface of the membrane (Seckler et al., 1983; Carrasco et al., 1984a,c).

(5) In proteoliposomes reconstituted with purified *lac* permease, both the 4B1 epitope and the C-terminus are accessible to the appropriate IgG, and binding of anti-C-terminal IgG is decreased by digesting the proteoliposomes with carboxypeptidase (Carrasco et al., 1984c; Seckler & Wright, 1984). Furthermore, neither the anti-C-terminal IgG nor carboxypeptidase digestion affects any of the transport reactions catalyzed by the permease. On the basis of these observations, it has been suggested (Carrasco et al., 1984c) that during reconstitution, the *lac* permease undergoes intramolecular dislocation of the ultimate C-terminus with no effect on its catalytic activity.

Although data are not presented, it is noteworthy that in addition to the partial cross-reactivity exhibited by the C-terminus and the 4A1OR epitope, antibody 4A1OR, like anti-C-terminal IgG, reacts with the *lac* permease in proteoliposomes but has no effect on any of its activities. Furthermore, digestion of the proteoliposomes with carboxypeptidases A and B leads to a decrease in binding of 4A1OR that parallels the decrease in binding of anti-C-terminal IgG. In view of these observations, it seems unlikely that the defect in 4A1OR binding observed in ML 308-22 vesicles reflects a change in the amino acid sequence of the ultimate C-terminus of the permease, since this region of the molecule seems to be totally unnecessary for catalytic activity. Rather, it seems more probable that the mutation alters an amino acid residue in another portion of the molecule with a secondary conformational change in the C-terminus that alters the binding of 4A1OR. On the other hand, if 4A1OR is directed against secondary or tertiary structure, and part of the epitope includes a portion of the C-terminus and part includes another portion of the molecule that is not continuous with the C-terminus, it is possible that this contiguous portion might contain the amino acid alteration encoded by the mutation. In other words, the results do not necessarily imply that the defect in the mutant permease (or the 4A1OR epitope) is in the ultimate C-terminus of the protein.

Added in Proof

Additional experiments have been performed recently with ^{125}I-labeled site-directed polyclonal antibodies directed against hydrophilic segments 5 (Glu^{130} to Phe^{145}) and 7 (Phe^{185} to Ala^{198}) [cf. Foster et al. (1983)]. As judged by binding experiments with ISO vesicles, anti-5 IgG binds 3-fold better to ML 308-22 vesicles relative to ML 308-225 vesicles, while anti-7 IgG binds only one-fourth as well. Clearly, therefore, these immunological probes are able to discriminate between wild-type and "uncoupled" permease molecules. In addition, the results suggest that the mutation causes a significant alteration in the conformation of the permease.

Registry No. TMG, 155-30-6; β-galactoside permease, 9063-67-6; proline, 147-85-3; hydrogen ion, 12408-02-5.

References

Barnes, E. M., Jr., & Kaback, H. R. (1971) *J. Biol. Chem. 246*, 5518.

Brooker, R. J., & Wilson, T. H. (1984) *Fed. Proc., Fed. Am. Soc. Exp. Biol. 43*, 1380.

Büchel, D. E., Groneborn, B., & Müller-Hill, B. (1980) *Nature (London) 283*, 541.

Carrasco, N., Tahara, S. M., Patel, L., Goldkorn, t., & Kaback, H. R. (1982) *Proc. Natl. Acad. Sci. U.S.A. 79*, 6894.

Carrasco, N., Tahara, S. M., Herzlinger, D., Viitanen, P., Goldkorn, T., Foster, D. L., & Kaback, H. R. (1983a) *Biophys. J. 41*, 383(a).

Carrasco, N., Herzlinger, D., & Kaback, H. R. (1983b) *Fed. Proc., Fed. Am. Soc. Exp. Biol. 42*, 7.

Carrasco, N., Herzlinger, D., DeChiara, S., Danho, W., Gabriel, T. F., & Kaback, H. R. (1984a) *Biophys. J. 45*, 83(a).

Carrasco, N., Viitanen, P., Herzlinger, D., & Kaback, H. R. (1984b) *Biochemistry 23*, 3681–3687.

Carrasco, N., Herzlinger, D., Mitchell, R., DeChiara, S., Danho, W., Gabriel, T. F., & Kaback, H. R. (1984c) *Proc. Natl. Acad. Sci. U.S.A. 81*, 4672.

Davis, B. D., & Mingioli, E. S. (1959) *J. Bacteriol. 60*, 17.

Felle, H., porter, J. S., Slayman, C. L., & Kaback, H. R. (1980) *Biochemistry 19*, 3585.

Foster, D. L., Boublik, M., & Kaback, H. R. (1983) *J. Biol. Chem. 258*, 31.

Garcia, M. L., Viitanen, P., Foster, D. L., & Kaback, H. R. (1983) *Biochemistry 22*, 2524.

Ghazi, A., & Shechter, E. (1981) *Biochim. Biophys. Acta 645*, 305.

Goldkorn, T., Rimon, G., & Kaback, H. R. (1983) *Proc. Natl. Acad. Sci. U.S.A. 80*, 3322.

Goldkorn, T., Rimon, G., Kempner, E. S., & Kaback, H. R. (1984) *Proc. Natl. Acad. Sci. U.S.A. 81*, 1021.

Herzlinger, D., Viitanen, P., Carrasco, N., & Kaback, H. R. (1984) *Biochemistry 23*, 3688–3693.

Hobson, A. C., Gho, D., & Müller-Hill, B. (1977) *J. Bacteriol. 131*, 830.

Kaback, H. R. (1968) *J. Biol. Chem. 243*, 3711.

Kaback, H. R. (1971) *Methods Enzymol. 22*, 99.

Kaback, H. R. (1974) *Methods Enzymol. 31*, 698.

Kaback, H. R. (1983) *J. Membr. Biol. 76*, 95.

Kaback, H. R. (1985) *Physiol. Membr. Disord.* (in press).

Kaczorowski, G. J., & Kaback, H. R. (1979) *Biochemistry 18*, 3691.

Kaczorowski, G. J., Robertson, D. E., & Kaback, H. R. (1979) *Biochemistry 18*, 3697.

Laemmli, U. K. (1970) *Nature (London) 227*, 680.

Lowry, O. H., Rosebrough, N. J., Farr, A. J., & Randall, R. J. (1951) *J. Biol. Chem. 193*, 265.

Newman, M. J., Foster, D., Wilson, T. H., & Kaback, H. R. (1981) *J. Biol. Chem. 256*, 11804.

Overath, P., & Wright, J. K. (1983) *Trends Biochem. Sci. (Pers. Ed.) 8*, 404.

Overath, P., Teather, R. M., Simoni, R. D., Aichele, G., & Wilhelm, U. (1979) *Biochemistry 18*, 1.

Patel, L., Garcia, M.-L., & Kaback, H. R. (1982) *Biochemistry 21*, 5805.

Ramos, S., Schuldiner, S., & Kaback, H. R. (1979) *Methods Enzymol. 55*, 680.

Reenstra, W. W., Patel, L., Rottenberg, H., & Kaback, H. R. (1980) *Biochemistry 19*, 1.

Robertson, D. E., Kaczorowski, G. J., Garcia, M.-L., & Kaback, H. R. (1980) *Biochemistry 19*, 5692.

Rudnick, G., Schuldiner, S., & Kaback, H. R. (1976) *Biochemistry 15*, 5126.

Schuldiner, S., Spencer, R. D., Weber, G., Weil, R., & Kaback, H. R. (1975) *J. Biol. Chem. 250*, 8893.

Seckler, R., & Wright, J. K. (1984) *Eur. J. Biochem. 142*, 269.

Seckler, R., Wright, J. K., & Overath, P. (1983) *J. Biol. Chem. 258*, 10817.

Short, S. A., Kaback, H. R., & Kohn, L. D. (1975) *J. Biol. Chem. 250*, 4291.

Trumble, W. R., Viitanen, P. V, Sarkar, H. K., Poonian, M. S., & Kaback, H. R. (1984) *Biochem. Biophys. Res. Commun. 119*, 860.
Viitanen, P., Garcia, M. L., Foster, D. L., Kaczorowski, G. J., & Kaback, H. R. (1983) *Biochemistry 22*, 2531.
Viitanen, P., Garcia, M. L., & Kaback, H. R. (1984) *Proc. Natl. Acad. Sci. U.S.A. 81*, 1629.
Waggoner, A. S. (1979) *Methods Enzymol. 55*, 689.
Watson, J. D. (1977) *The Molecular Biology of the Gene*, W. A. Benjamin, Menlo Park, CA.
West, I. C., & Wilson, T. H. (1973) *Biochem. Biophys. Res. Commun. 50*, 5551.
Wilson, T. H., & Kutsch, M. (1972) *Biochim. Biophys. Acta 255*, 786.
Wong, P. T. S., Kashket, E. R., & Wilson, T. H. (1970) *Proc. Natl. Acad. Sci. U.S.A. 65*, 63.

Truncated Repeated Sequences Generated by Recombination in a Specific Region

Francine C. Eden*

Laboratory of Molecular Carcinogenesis, National Cancer Institute, National Institutes of Health, Bethesda, Maryland 20205
Received March 8, 1984

ABSTRACT: Structural relationships within a family of long repeated DNA sequences have been determined by molecular cloning of individual family members. About half of the family members are truncated at one end. There is a short, tandemly repeating region flanked by direct repeats associated with truncation. Recombination in a region near the tandemly repeating segment has apparently generated much of the diversity in this family.

For the vast majority of families of repeated DNA sequences, the structural relationships among family members have not been determined beyond the basic fact that they can base pair with reasonable fidelity. Through molecular cloning, these relationships are beginning to be explored. In some instances, the data go beyond description of a particular family to suggest mechanisms whereby families originate, incur variability, and are dispersed in the genome [reviewed by Brutlag (1980), Jelinek & Schmid (1982), and Singer (1982)].

In rodent genomes, there are families of long repeated DNA sequences some of whose members are truncated at the 5′ end (Fanning, 1983; Gebhard et al., 1982; Wilson of Storb, 1983). The presence of a poly(A) stretch at the 3′ boundary of these elements suggests a mechanism whereby truncated variants could be generated. The steps would be (1) RNA transcription beginning or ending internal to the element, (2) polyadenylation, (3) reverse transcription, and (4) reintegration of the shortened DNA copy. Mechanisms involving RNA intermediates may also be responsible for the structure and dispersal of short repeated sequence families like the Alu family and for the generation of processed genes and pseudogenes (Jagadeeswaran et al., 1981; Van Arsdell et al., 1981; Sharp, 1983). Thus, the repeated component of the genome seems to incur variability by some of the same mechanisms that generate change within structural genes.

Here a family of chicken repeated DNA sequences is described where some members are apparently shortened at one end. This family, which has been studied previously by molecular cloning of individual family members and by genomic blotting (Eden et al., 1980, 1981; Musti et al., 1981), has about 500 genomic copies, each several kilobases in length. In the chicken genome, large repetitive regions occur where an individual member of this family is clustered with other long repeated sequences. The family includes structural variants distinguishable by restriction analysis. It has now been determined how some of this variability arose. A short, tandemly repeating region has been discovered within some family members. It is apparently associated with a specific region of recombination responsible for truncation of some family members at one end.

* Correspondence should be addressed to this author at Meloy Laboratories, 6715 Electronic Drive, Springfield, VA 22151.

Experimental Procedures

Cloned DNA Segments. A 3.6-kilobase (kb)[1] *Eco*RI fragment of chicken DNA cloned in the plasmid pBR322 represents one member of a family of long repeated sequences (Eden et al., 1980) and was used as a source of probes for all of this work. The segments derived from it (Figure 1) were isolated either by separation of restriction fragments in agarose or acrylamide gels (probes I, IV, V, and VI) or by recloning in pBR322 (probes II and III). Recombinant phages containing sequences homologous to the 3.6-kb fragment were selected by screening a library of chicken DNA prepared and provided by D. Engel. It was constructed by the method of Maniatis et al. (1978). Positive phases were plaque purified twice prior to amplification and DNA isolation. Phage and plasmid DNAs were prepared as described previously (Eden et al., 1980).

DNA Labeling and Sequencing. DNA used in hybridization experiments was labeled with ^{32}P by nick translation (Rigby et al., 1977). End labeling of DNA was performed by addition of [γ-^{32}P]ATP to dephosphorylated termini using T4 polynucleotide kinase. DNA sequencing was performed according

[1] Abbreviations: SSC, 0.15 M NaCl and 0.015 M trisodium citrate; SDS, sodium dodecyl sulfate; kb, kilobase; bp, base pair; EDTA, ethylenediaminetetraacetic acid.